Field Crops Research 300 (2023) 109010

Contents lists available at ScienceDirect

Field Crops Research

journal homepage: www.elsevier.com/locate/fcr

A high-yield and high-efficiency cultivation pattern of winter wheat in North China Plain: High-low seedbed cultivation

Zhuanyun Si [a,1], Junming Liu [a,b,1], Lifeng Wu [c], Sen Li [a], Guangshuai Wang [a], Jiachuan Yu [c], Yang Gao [a,*], Aiwang Duan [a,*]

[a] Institute of Farmland Irrigation, Chinese Academy of Agricultural Sciences, Xinxiang, Henan 453002, PR China
[b] Graduate School of Chinese Academy of Agricultural Sciences, Beijing 100081, PR China
[c] Binzhou Academy of Agricultural Sciences, Binzhou, Shandong 256600, PR China

ARTICLE INFO

Keywords:
High-low seedbed cultivation
Winter wheat
Grain yield
Water use efficiency
Nitrogen use efficiency

ABSTRACT

Context: Traditional cultivation pattern (TC) of winter wheat has shortages of insufficient land utilization and low water and nitrogen use efficiency, which restrict the sustainability of wheat production in the North China Plain (NCP).

Research question: A new planting pattern of high-low seedbed cultivation (HLSC) was developed to increase land utilization rate and wheat productivity. However, the mechanisms of grain yield and water-nitrogen use efficiency increase under the HLSC pattern are not well understood.

Methods: Therefore, we conducted a three-year (2017–2020) field experiment to explore the effects of cultivation patterns on the distribution of soil water and nitrite, plant growth, grain yield, and water-nitrogen use efficiency under different irrigation levels by employing TC and HLSC patterns.

Results: Results showed that the HLSC pattern significantly promoted grain yield, water use efficiency of grain (WUE_G), and nitrogen use efficiency (NUE) of winter wheat under different irrigation levels. Across three irrigation levels, HLSC significantly increased grain yield by 22.63%, 10.30%, and 9.96% in the three seasons, respectively, compared to TC. The higher grain yield under HLSC was ascribed mainly to the increases in effective spike number, which produced more LAI and aboveground biomass. Although wheat under HLSC consumed more water, the WUE_G across irrigation levels under HLSC was 6.77%, 2.38%, and 4.28% higher than those under TC for the three seasons, due to the reduction of ineffective soil surface evaporation under HLSC. Moreover, HLSC stimulated roots to uptake more water stored in the subsoil layer, which was conducive to developing a larger soil reservoir capacity for storing rainwater in summer. Wheat plants under HLSC absorbed 21.76% more nitrogen and finally achieved an average 14.29% increase of NUE over the irrigation levels and seasons. Principal component analysis (PCA) revealed that HLSC is recommended as the best cultivation in wheat production.

Conclusions: The results suggest that HLSC is a promising cultivation pattern for improving grain yield and water-nitrogen use efficiency in winter wheat production in the NCP.

Significance: Our study provides a practical reference to explore sustainable cultivation patterns of winter wheat in areas with similar climate conditions to the NCP.

1. Introduction

Food security is a major challenge facing mankind in the 21st century (Pergner and Lippert, 2023), and this challenge is likely to increase in the context of climate change and growing competition for natural resources (Cassman and Grassini, 2020). Studies show that by 2050, food production must increase by 60–110% (from 2005) to meet growing demand (van Dijk et al., 2021; Guarin et al., 2022). Increasing production by expanding agricultural land requires high human and environmental costs (Qi et al., 2018), so high-yield and efficient agriculture must be developed to achieve the necessary production benefits on existing farmland. The North China Plain (NCP) is an important grain

* Corresponding authors.
E-mail addresses: gaoyang@caas.cn (Y. Gao), duanaiwang@aliyun.com (A. Duan).
[1] These authors contributed equally to this work

https://doi.org/10.1016/j.fcr.2023.109010
Received 21 November 2022; Received in revised form 5 June 2023; Accepted 13 June 2023
Available online 20 June 2023

production base in China (Du et al., 2014), in which the wheat output accounts for about 70% of the total national output (Liu et al., 2023b). Therefore, improving winter wheat production in this region is of great significance to China's food security.

In the NCP, due to the low rainfall during the winter wheat growing season, high and stable yields are highly dependent on irrigation (Jha et al., 2019; Zhang et al., 2022). At present, surface irrigation is still the dominant irrigation pattern for winter wheat in North China, accounting for more than 85% of the total irrigated area (Ministry of Water Conservancy, 2017). Although the main irrigation system has been greatly improved through water-saving reconstruction in large-scale and medium-scale irrigated areas in the last decades, the improvement of the field water distribution system is still very limited. Traditionally, farmers built borders in the fields, dividing them into many narrow beds and irrigating them with flood irrigation within the boundary basins (Wang et al., 2004; Liu et al., 2020). Because some spaces are reserved necessarily for building the borders, the traditional cultivation pattern (TC) leads to insufficient land utilization and some loss of effective light interception, resulting in a decrease of wheat grain yield (Wu et al., 2021). In addition, the TC pattern tends to lead to poor ventilation and light transmission in the middle and lower part of the plant population, which is not conducive to the improvement of population photosynthesis and wheat stress resistance (Wang et al., 2004; Du et al., 2021b).

To address this challenge, high-low seed bed cultivation (HLSC) was developed and have been widely used in crop production on the Shandong province, China (Wu et al., 2021). In HLSC, the high bed (HLSC-H) effectively eliminates the border of TC and forms a wavy canopy structure, which may be beneficial to the growth and development of wheat (Du et al., 2021a). A relevant study has reported that HLSC offers multiple advantages, including forming an ideal canopy structure,

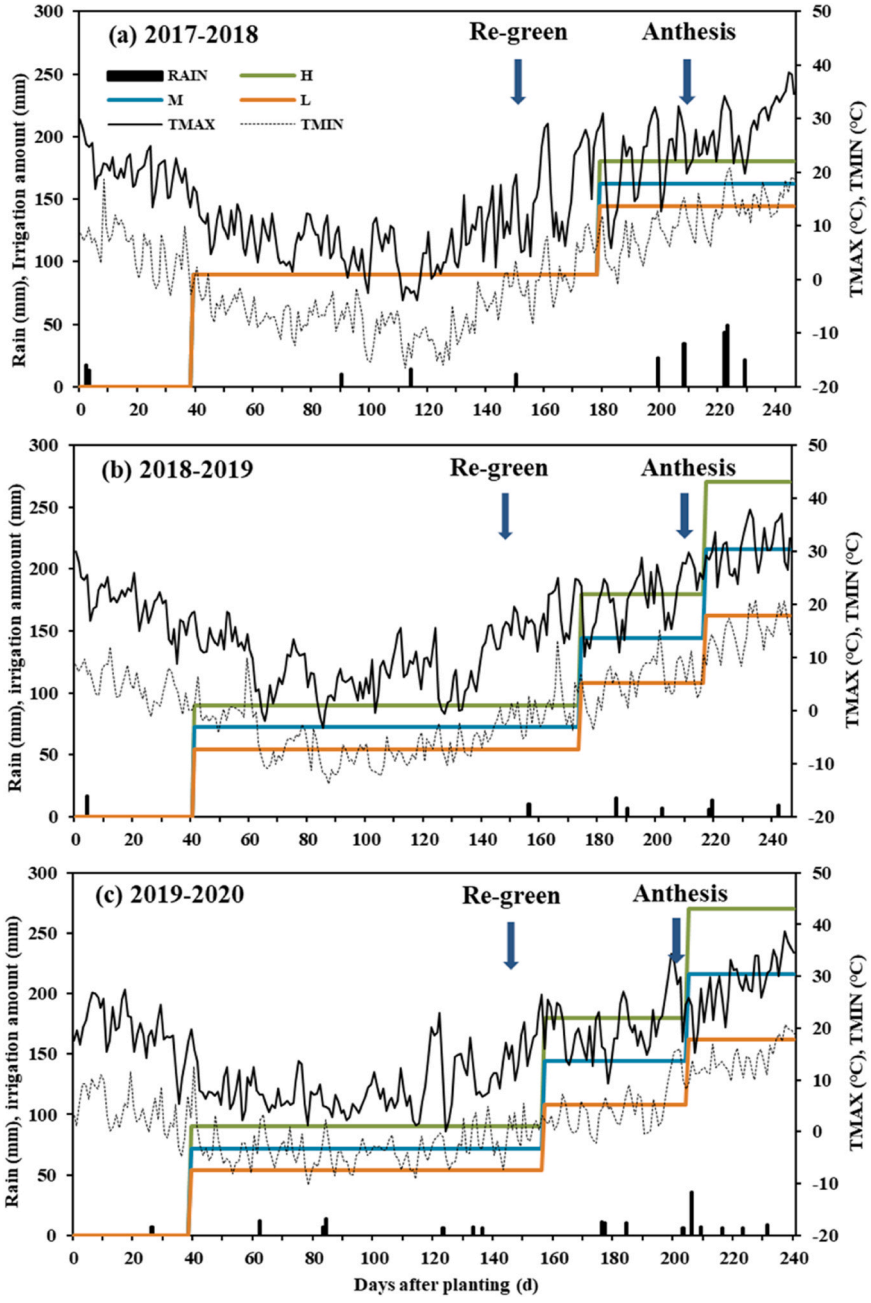

Fig. 1. Daily rainfall (RAIN), maximum temperature (TMAX), minimum temperature (TMIN), and accumulation irrigation amount of different treatments during the three winter wheat seasons. Note: H, M, and L mean full irrigation, mild deficit irrigation, and deficit irrigation, respectively.

enhancing grain yield, and improving lodging resistance (Wu et al., 2021). However, the characteristics of resource use, particularly water and nitrogen use, in HLSC cultivation have not been well studied. The lack of knowledge may restrict the further improvement and wider application of the HLSC pattern. In addition, in agricultural production practice, winter wheat growth often goes through various soil water situations, and soil moisture is an important factor affecting root water and nitrogen uptake and crop growth. Therefore, the influence of different soil water conditions should be considered when studying the regulatory effects of different cultivation patterns in the future.

The objectives of this study were to (i) investigate the characteristics of soil water and nitrite distribution, wheat growth, crop water consumption, and plant N absorption of different cultivation patterns under different irrigation levels and (ii) analyze the mechanisms influencing grain yield, water and nitrogen use efficiency of different cultivation methods. (iii) determine the appropriate cultivation pattern in the study area. The results will be helpful to explore high-yield and high-efficiency cultivation patterns in the NCP.

2. Materials and methods

2.1. Experimental site

The experiments were conducted during the 2017–2018, 2018–2019, and 2019–2020 wheat growing seasons at the field experimental station of Binzhou Academy of Agricultural located in Dianzi Town, Boxing County, Shandong Province (118.29°E, 37.06°N). The station belongs to the Yellow River Alluvial Plain, a very important winter wheat production area in China, and a temperate continental monsoon climate area with average annual precipitation of 589 ± 146.4 mm, a mean temperature of 13.4 ± 0.5 ℃. The daily precipitation, maximum temperature, and minimum temperature during the three seasons are shown in Fig. 1. The rainfall amount during the growth period of winter wheat during 2017–2018, 2018–2019, and 2019–2020 are 253.5, 95.5, and 162.7 mm, respectively. The soil type in the field is silty loam with a bulk density of 1.50 g cm^{-3}. Detailed soil physical parameters in the 0–100 cm soil layer and chemical properties in the 0–40 cm layer are shown in Table S1 and Table S2, respectively.

2.2. Experimental design

The field experiment was designed in a split-plot arrangement consisting of two experimental factors. The main plot was arranged for two cultivation patterns: (1) traditional cultivation (TC): consisted of all plane seedbeds of 120 cm wide, separated by ridges of 30 cm wide; four rows of wheat were sown on the seedbeds at an average spacing of 30 cm, and irrigation water and topdressing fertilizers were applied uniformly in the entire seedbed (Fig. 2a). (2) High-low seedbed cultivation (HLSC): consisted of low seedbeds of 90 cm wide, separated by raised seedbeds of 60 cm wide; four rows of wheat were sown on the low bed and two rows on the raised bed (Fig. 2b). The irrigation and topdressing fertilizer were performed in the low bed of HLSC (HLSC-L) (Fig. 2).

The subplot was arranged with three irrigation quotas of 90, 72, and 54 mm, respecting full irrigation treatment (H), mild deficit irrigation treatment (M), and severe deficit irrigation treatment (L), respectively. In the 2017–2018 season, only full irrigation treatment was set in TC. When the average SWC of 0–100 cm soil layer in full irrigation treatment decreased to 55%− 60% of the field water capacity, irrigation was carried out in all three irrigation treatments with arranged water quota. Fig. 1 shows the irrigation time and total irrigation amount under the three irrigation treatment levels. The two cultivation patterns and the three irrigation quotas interacted as 6 experimental treatments (4 treatments in the 2017–2018 season). Three plots of 180 m^2 (9 m × 20 m) were arranged to implement the 3 replications.

Wheat variety Jimai-22 was used in the 2017–2018 season, and Jimai-23 in the 2018–2019 and 2019–2020 seasons due to local large-scale wheat variety alternatives. Previous study and large-scale application found that Jimai-23 improved quality and resistance to powdery mildew, and other characteristics were similar to Jimai-22 (Jia et al., 2020). This ensures that the findings in this paper will not be affected by variety choice. The wheat was sown on October 5, and harvested on June 8, in the 2017–2018 and 2018–2019 seasons. In the 2019–2020 season, the wheat was sown on October 15 and harvested on June 8. The seed amounts sowed for the two cultivation patterns was the same as 120 kg ha^{-1} to ensure the same initial number of seedlings per area. The basal fertilizers consisting of 120 kg ha^{-1} N (Urea), 120 kg ha^{-1} P (P_2O_5), and 120 kg ha^{-1} K (in K_2O) were applied justly before sowing. The topdressing N of 120 kg ha^{-1} was applied on April 2, 2018, March 28, 2019, and March 19, 2020, respectively.

2.3. Sampling and measurements

2.3.1. Soil sampling

Justly before sowing and after harvesting, soil samples were taken at 0–10, 10–20, 20–30, 30–40, 40–60, 60–80, 80–100, 100–120, and 120–150 cm soil depth increment using an auger. For HLSC, the soil was sampled in both high beds (HLSC-H) and low beds (HLSC-L). Each fresh soil sample was divided into two parts. One part was placed in aluminum cans and dried at 105 °C to a constant weight and used to determine SWC. Another part was quickly pocketed in plastic bags and then stored in a 4 ℃ refrigerator for further analysis. NO_3-N was extracted using 2 mol L^{-1} KCl solution and measured using an AA3 flow analyzer (Seal Analytical Inc. AA3-HR USA). Soil water storage (SWS, mm) in the soil at harvest was calculated according to Eq. (1):

$$SWS = \sum_{1}^{n} h_i \times \rho_i \times b_i \times 10 \quad (1)$$

where, h_i is the thickness of the i^{th} soil layer, cm; ρ_i is the soil bulk density of the i^{th} soil layer, (g cm^{-3}). b_i is the SWC of the i^{th} soil layer; n is the number of soil layers divided for sampling.

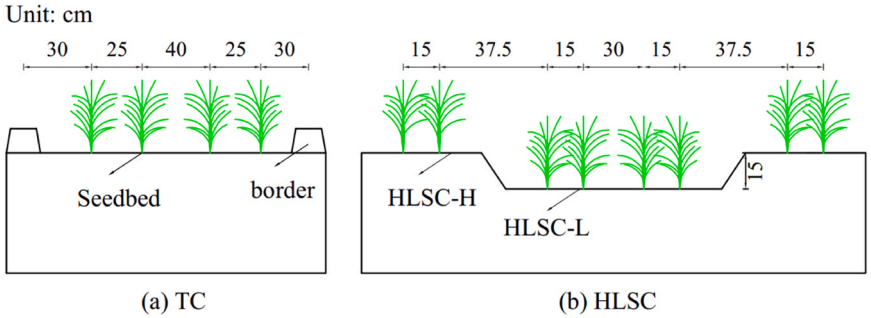

Fig. 2. Traditional cultivation (TC) and high-low seedbed cultivation (HLSC). The irrigation and topdressing fertilizer were performed in the seedbed of TC and the low bed of HLSC (HLSC-L).

Crop evapotranspiration (ET_a, mm) was calculated using the soil water balance equation as follows (Si et al., 2020):

$$ET_a = \Delta S + P + I + U - R - D_W \quad (2)$$

where ΔS (mm) is the change of soil water storage, P (mm) is precipitation, I (mm) is irrigation amount, U(mm) is upward capillary flow into the 0–150 cm zone, R (mm) is the surface runoff, D_W (mm) is the downward drainage out the 0–150 cm zone. U was negligible due to the deep groundwater level, and the measured values of R and D_W were zero during the three growing seasons.

2.3.2. Plant sampling

Plants number per meter was measured from the labeled 1 m length of sampling section before tillering (about 30 days after sowing), and every 10–15 days during the re-green stage to harvest, and then converted to plant density according to the previous study (Jha et al., 2019).

Leaf area index (LAI) and aboveground biomass were manually measured by taking randomly plants as samples. For the TC, samples were taken from both the side row and the inside row, then mixed. Leaf length and themaximum width of each leaf on 10 sampled plants were measured with a ruler, and the LAI was calculated using the method described in the previous study (Jha et al., 2019). The 40 sampled plants were then dried in an oven at 75 ℃ until reaching a constant weight and weighed for calculating the aboveground biomass following Jha et al. (2019). For the HLSC, plant samples were taken from high and low beds, respectively. LAI and biomass per area were calculated using a weighted average (2:4 based on high: low rows).

2.3.3. Total nitrogen content in plants

The main organs (stem, leaf, and ear) of sample plants were separated, dried, and weighed respectively, and then used to measure total nitrogen content. The measuring method may be described as follows: the dried organ was ground and crushed, sifted with a 0.5 mm screen, boiled with H_2SO_4-H_2O_2, and then determined total nitrogen content was by AA3 flow analyzer (Seal Analytical Inc. AA3-HR USA). Nitrogen uptake of an organ was calculated by multiplying the dry weight of the organ and its total nitrogen content. Nitrogen uptake of a single plant was considered as the total nitrogen uptakes of all organs, and nitrogen accumulation of the population was obtained by multiplying the average nutrient uptake of the single plant by population density.

2.3.4. Grain yield and its compositions

Grain yield was determined from a 1.5 m^2 undisturbed area in the middle of each plot. All grains were air-dried naturally with 13% water content, weighed, and the values are converted to the final yield. In each plot, the one meter row was counted for measuring the spike number. For the HLSC, the plants in the raised and low beds were counted respectively, and the spike number per area was calculated by weighted average. Forty plants of each plot were randomly collected for measuring kernels per spike. The 1000-grain weight (with 13% water content) was calculated by weighing 1000 seeds taken randomly from the yield measurement sample.

2.3.5. Water and nitrogen use efficiencies

Water use efficiency of grain (WUE_G, kg m^{-3}), water use efficiency of aboveground biomass (WUE_{AB}, kg m^{-3}), nitrogen use efficiency (NUE, kg kg^{-1}), nitrogen uptake efficiency (NupE, kg kg^{-1}), and nitrogen utilization efficiency (NutE, kg kg^{-1}) were calculated with Eqs. (3), (4), (5), (6), and (7).

$$WUE_G = 0.1\frac{Y}{ET_a} \quad (3)$$

$$WUE_{AB} = 0.1\frac{\text{Aboveground Biomass}}{ET_a} \quad (4)$$

$$NUE = \frac{Y}{N_s} \times 100\% \quad (5)$$

$$NupE = \frac{N_t}{N_s} \times 100\% \quad (6)$$

$$NutE = \frac{Y}{Nt} \times 100\% \quad (7)$$

where, Y (kg ha^{-1}) is grain yield, ET_a (mm) is actual evapotranspiration, N_s (kg ha^{-1}) is nitrogen application rate, and N_t (kg ha^{-1}) is the total nitrogen uptake at maturity.

2.4. Statistical analysis

The effects of cultivation pattern and irrigation level on wheat growth, grain yield, WUE_G, WUE_{AB}, and NUE were assessed by two-factor analysis of variance (ANOVA) using SPSS 24.0. Significant differences among treatments were assessed using Duncan's multiple range test at the 5% level. The plant number measured repeatedly was tested by repeated measurement variance analysis and Mauchly's Test of Sphericity. The correlation relationships between grain yield and growth traits were analyzed using Pearson's correlation coefficients. PCA was used to analyze grain yield, aboveground biomass, 1000-grain weight, kernels per spike, spike number, ET, N_t, WUE_G and NupE as influenced by the cultivation pattern and irrigation level.

3. Results

3.1. Distribution of water and NO_3-N in soil profiles

SWC in the 0–150 cm soil profiles varied with soil depths, cultivation patterns, and irrigation amount levels on the fifth day after irrigation and fertilization at the jointing stage in three seasons (Fig. 3). SWC of the topsoil (0–10 cm) in the high bed (HLSC-H) was significantly lower than that in the low bed (HLSC-L) under three irrigation levels. For example, the averaged SWC in 0–10 cm of HLSC-L in the 2018–2019 season was 19.22%, across all irrigation levels, while that of HLSC-H was 15.34% (Fig. 3). Fig. S1 showed the actual SWC distribution under HLSC patterns after irrigation. It was found that the surface soil of HLSC-H is still in a relatively dry state after irrigation. At the same time, it also was found that underneath the topsoil, SWC values are nearly the same in the same depth soil layers for HLSC-H and HLSC-L under three irrigation levels (Fig. 3). This indicated that although the irrigation mode of HLSC belongs to local irrigation, soil water distribution modes in the middle and deep soil layers beneath different seedbeds are consistent after irrigation water infiltration and redistribution. Under the same cultivation pattern, the average SWC in 0–150 cm soil profile increased with the increase in irrigation amount.

Fig. 4 shows the distribution of soil NO_3-N on the fifth day after irrigation and nitrogen application. Soil NO_3-N was mainly concentrated in the 0–60 cm soil layer under the two cultivation patterns. Soil NO_3-N was the largest in the 10–20 cm soil layer, and then gradually decreased with the increase of depth. There was no significant difference in soil NO_3-N in different soil layers below 60 cm, which was at a low level. Under the HLSC pattern, the soil NO_3-N of HLSC-H was significantly lower than that of HLSC-L in the same soil layer for three irrigation levels. For example, soil NO_3-N of HLSC-H and HLSC-L in the 0–60 cm soil layer were 7.09 and 13.77 mg kg^{-1}, respectively, across irrigation levels in the 2018–2019 season. This may be contributed to that topdressing nitrogen was only applied to the low beds under the HLSC, resulting in a higher NO_3-N in the low-bed soil. Irrigation level seemed to have no significant effect on the distribution of soil NO_3-N. The distribution of soil NO_3-N under different irrigation levels was the same under the same cultivation mode.

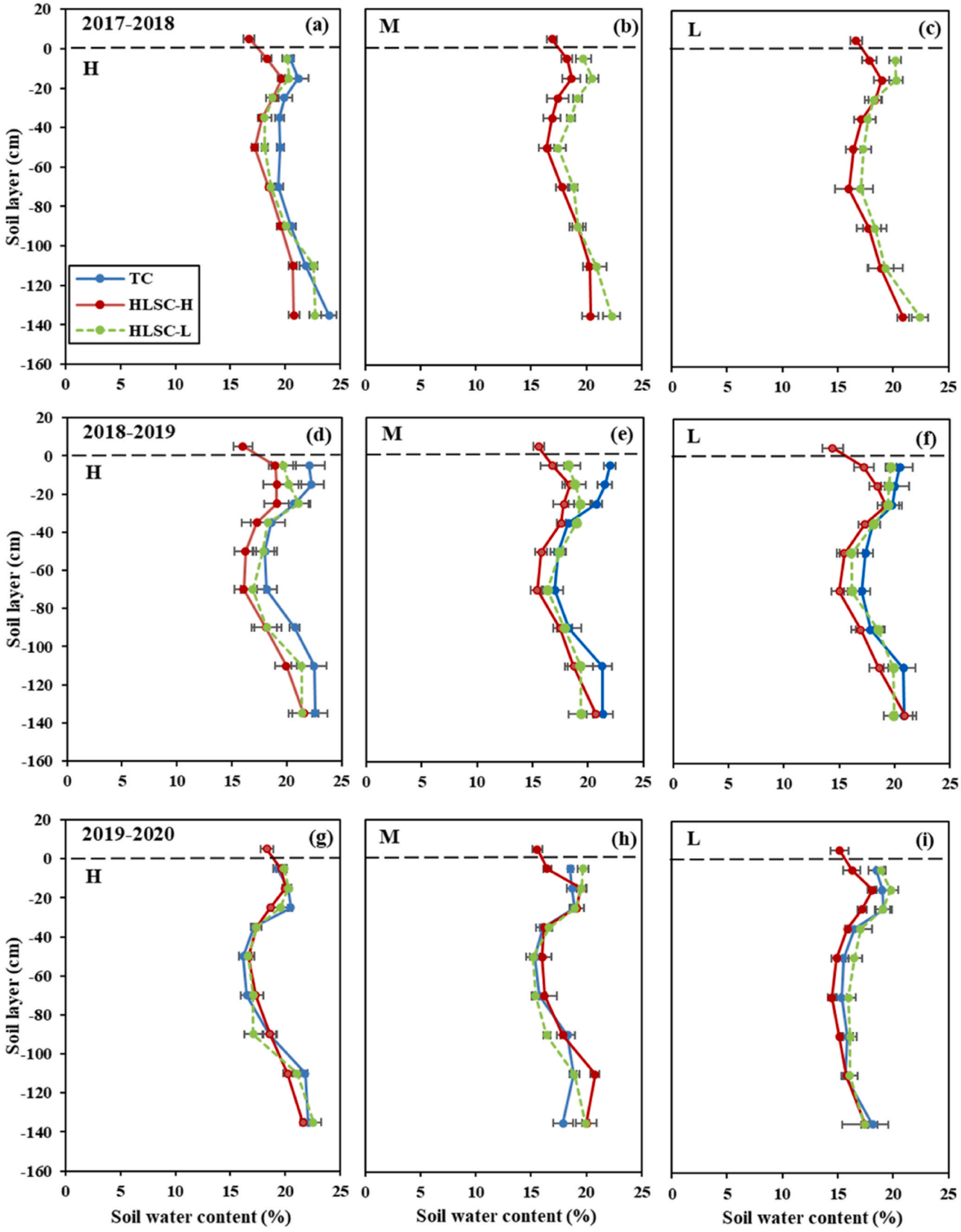

Fig. 3. Soil water content (%) distribution in 0–150 cm soil profile on the fifth day after irrigation and fertilization under different treatments in the 2017–2018, 2018–2019, and 2019–2020 seasons. Note: Data are presented as the means of three replicates ± SE (n = 3). HLSC-H and HLSC-L mean the high bed and low bed of the HLSC method, respectively. H, M, and L mean full irrigation, mild deficit irrigation, and deficit irrigation, respectively.

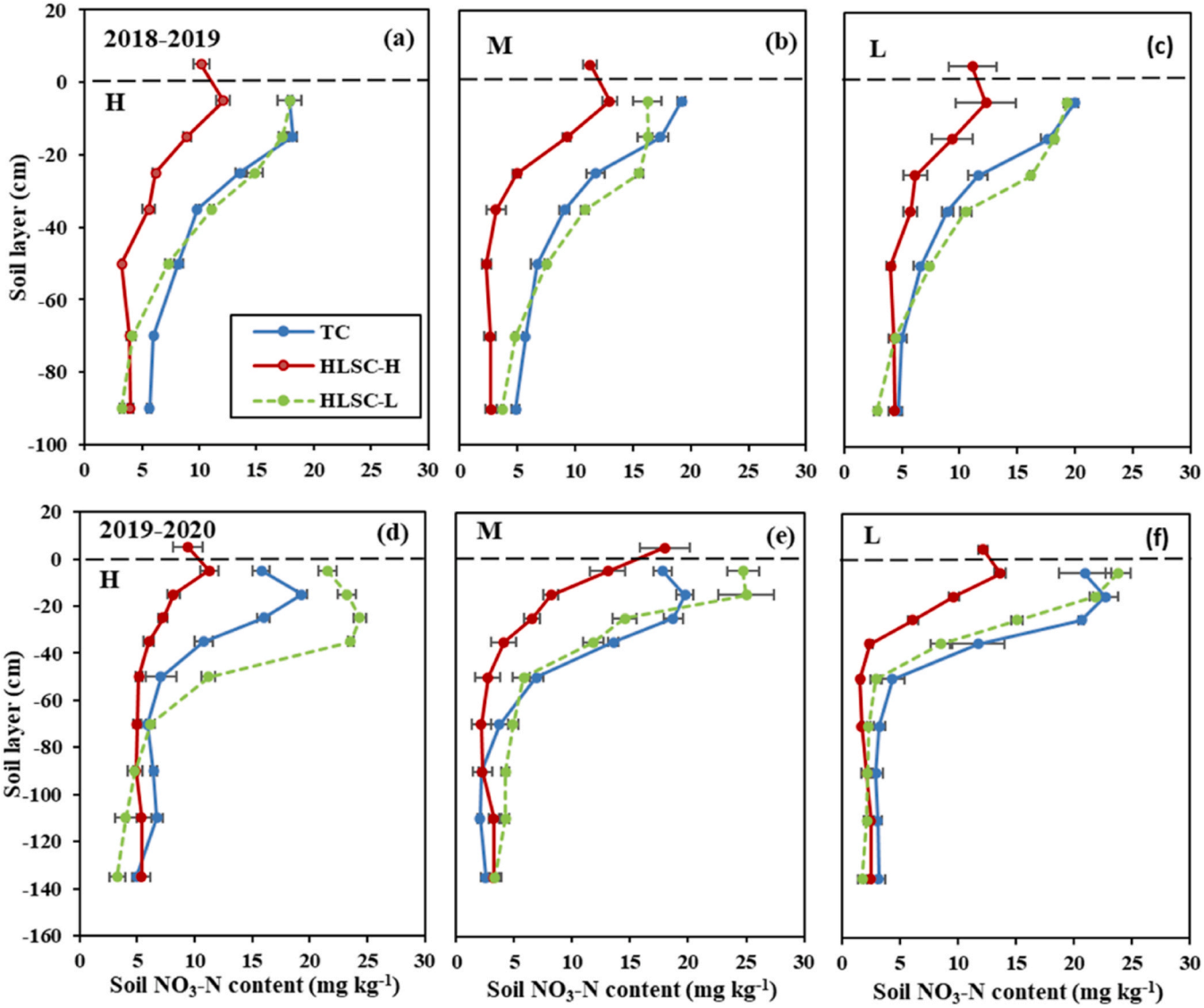

Fig. 4. The soil NO_3-N content (mg kg^{-1}) distribution in 0–150 cm soil profile on the fifth day after irrigation and fertilization under various treatments in the 2018–2019 and 2019–2020 seasons. Note: Data are presented as the means of three replicates ± SE (n = 3). HLSC-H and HLSC-L mean the high bed and low bed of the HLSC method, respectively. H, M, and L mean full irrigation, mild deficit irrigation, and deficit irrigation, respectively.

3.2. Plant density, LAI, and aboveground biomass

Table S3 showed that the wheat number data in 2017–2018 met the spherical hypothesis test ($P = 0.603$), while the data in 2018–2019 and 2019–2020 did not meet the spherical hypothesis test ($P = 0.01$ and $P = 0.009$), so within-subjects effect tests and multivariate tests were used, respectively. Sampling time and cultivation pattern had significant influence on wheat plant number, while irrigation method had significant influence on wheat plant number only in 2018–2019 season (Table S3). Due to the same sowing amount of the two cultivation patterns, there were no significant differences in the number of wheat plants before tillering (about 30 days after sowing) between the two cultivation patterns. The wheat plant density in 2018–2019 and 2019–2020 was about 1.9 and 1.8 million plants/ha before tillering, respectively (Fig. 5). Wheat number reached the maximum when the accumulated growing degree day (AGDD) reaches about 427–555 ℃·d, and then decreased with part tillers withering away. Wheat numbers were notably different under two cultivation patterns after the AGDD exceed 400 ℃·d, and the number of HLSC was significantly higher than that of TC under different irrigation levels. Across irrigation levels, the plant number at maturity under the HLSC method was 33.11%, 15.19%, and 47.50% higher than those under TC in the 2017–2018, 2018–2019, and 2019–2020 seasons, respectively. The plant number increased gradually with the increase of irrigation amount after the re-green stage, and the maximum values are investigated at full irrigation treatment.

As shown in Table 1, both the cultivation pattern and irrigation level significantly affected the LAI and aboveground biomass of winter wheat at the anthesis stage, where their interaction effects were not significant difference, except for individual years. Under the same irrigation level, LAI and aboveground biomass of HLSC were significantly higher than those of TC (Table S4). Across irrigation levels, the LAI of HLSC increased by 27.37%, 12.95%, and 48.84% in three seasons, respectively, compared with TC. The aboveground biomass under HLSC was 35.58%, 24.38%, and 46.78% higher than those under the TC pattern, respectively. Similarly, under the same cultivation pattern, LAI and aboveground biomass increased gradually with the increase of irrigation quota and reached the maximum value under full irrigation treatment. It was recorded that winter wheat was affected by late spring cold in 2017–2018, resulting in significantly lower LAI and aboveground biomass than those in 2018–2019 and 2019–2020. The greatest LAI and

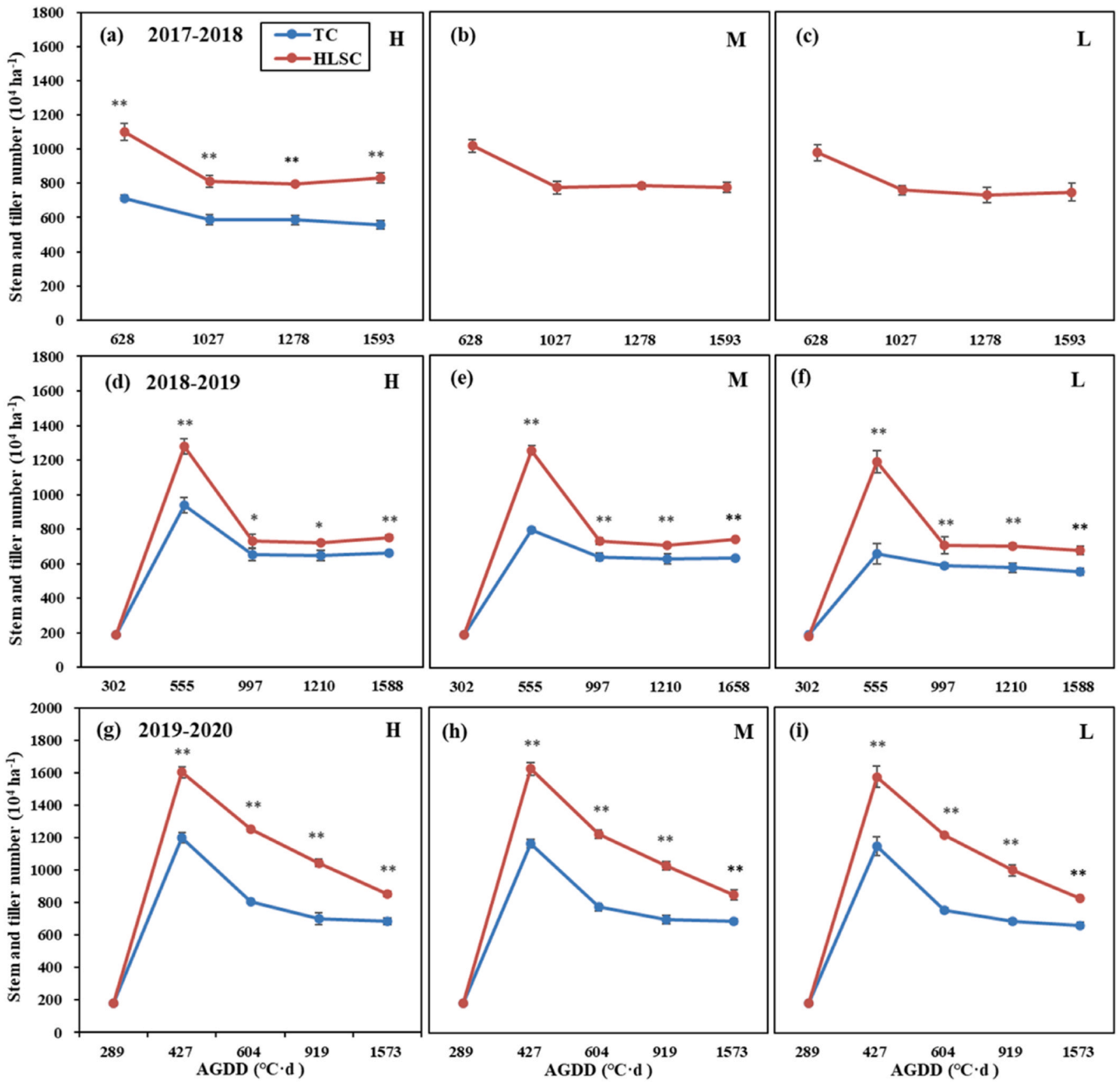

Fig. 5. The winter wheat plant number under different cultivation patterns and irrigation levels in the 2017–2018, 2018–2019, and 2019–2020 seasons.Note: H, M, and L mean full irrigation, mild deficit irrigation, and deficit irrigation, respectively. AGDD respects accumulated growing degree day. * * indicates significant differences within a cultivation pattern at $P < 0.01$. * indicates significant differences within a planting pattern at $P < 0.05$.

Table 1
Analysis of variance showing the effects of the cultivation pattern, irrigation level and their interaction on the leaf area index (LAI) and aboveground biomass of winter wheat at anthesis stage in the 2017–2018 – 2019–2020 growing seasons.

ANOVA	LAI			Aboveground biomass		
	2017–2018	2018–2019	2019–2020	2017–2018	2018–2019	2019–2020
C	**	**	**	**	**	**
I	NS	**	*	*	**	NS
C×I	-	NS	NS	-	**	NS

Note: C means cultivation methods, I means irrigation levels, and C×I means the interaction effect of two factors. * * Significant differences at $P < 0.01$; *Significant differences at $P < 0.05$; NS means no significant difference.

aboveground biomass values occurred under full irrigation treatment of HLSC and were 5.09, 6.22, and 6.28 for LAI and 10,832, 12,668, and 15,026 kg ha^{-1} for aboveground biomass in 2017–2018, 2018–2019, and 2019–2020 growing seasons, respectively.

3.3. Grain yield and composition

The grain yield of HLSC was significantly higher than those of TC under three irrigation levels and recorded as increasing 22.63%, 10.30%, and 9.96% in the 2017–2018, 2018–2019, and 2019–2020 seasons, respectively, across irrigation levels (Table 2). The effects of irrigation level on yield reached a significant level ($P < 0.05$) only in 2018–2019 (Table 3). The grain yield declined with the decrease in irrigation quota under the two cultivation patterns. The interaction between cultivation mode and irrigation level had no significant effects on yield (Table 3). The spike density, kernels per spike, and 1000-grain weight are the three main factors constituting wheat yield. The spike density of HLSC was significantly higher than that of TC under three irrigation levels, with maximum spike densities of HLSC recorded as 7.78, 7.53, and 8.52 million per hectare in the three seasons, across irrigation levels. With the decrease in irrigation quota, the spike densities decreased under the same cultivation pattern, and a significant difference was investigated among the three irrigation treatments only in 2018–2019. The significant effects of cultivation patterns on grain number per spike and 1000-grain weight were not recorded. The spike number, grain number per spike, 1000-grain weight, and grain yield of winter wheat in the 2017–2018 seasons were significantly lower than those in the 2018–2019 and 2019–2020 seasons, which may be attributed to the late spring cold in 2017–2018. The climatic event affected wheat vegetable development, grain formation, and the final grain yield.

3.4. Water consumption and water use efficiency

As shown in Table 4, both the cultivation pattern and irrigation level significantly affected the ET_a and soil water depletion, where their interaction effects were no significant difference, except in 2018–2019. The ET_a ranged from 464.2 to 575.7 mm, 445.7 to 571.2 mm, and 461.8 to 526.3 mm for different treatments in 2017–2018, 2018–2019, and 2019–2020, respectively. It can be found that more irrigation water is required, and more soil water storage is consumed in growing seasons with less rainfall. Across irrigation levels, the average ET_a of HLSC was 551.5, 529.7, and 509.6 mm, and 14.16%, 7.71%, and 5.45% higher than those of TC pattern in 2017–2018, 2018–2019, and 2019–2020 seasons, respectively. Similarly, the soil water depletion in the wheat field under HLSC is greater than those under TC. Soil water depletion under the HLSC pattern was 79.88%, 19.93%, and 25.16% higher than those under the TC pattern in the three seasons, respectively. Under the same cultivation mode, ET_a increased with the increase of irrigation amount, and the maximum ET_a was measured in full irrigation treatment.

Across irrigation levels, the WUE_{AB} of HLSC was 22.03%, 22.65%, and 23.47% higher than those of TC, respectively (Table S5). Similar to WUE_{AB}, the WUE_G of HLSC was also higher than that of TC in all irrigation levels, but only the difference between the two patterns in the 2017–2018 season reached a significant level (Table 4). These results indicated that winter wheat under HLSC can produce more biomass and grain yield per unit of water consumption. Under the same cultivation pattern, WUE_G and WUE_{AB} tended to decrease with the increase of irrigation amount and reached peak values in medium water and low water treatment. Under all treatments, the WUE_G and WUE_{AB} in 2017–2018 were lower than those in 2018–2019 and 2019–2020, because a severe freezing injury resulted in notable grain yield and biomass losses in the 2017–2018 season.

3.5. Total nitrogen uptake (N_t), nitrogen use efficiency (NUE), nitrogen uptake efficiency (NupE), and nitrogen utilization efficiency (NutE)

The N_t of HLSC was significantly higher than those of TC under three irrigation levels (Table S6). Increasing irrigation amount had to promote effects on N_t, but only the results in the 2018–2019 season reached a significant level (Table 5). Similarly, NUE and NupE were significantly affected by cultivation patterns, but no significant difference was observed in irrigation levels, except in 2018–2019. The average NUE (NupE) cross-irrigation levels under HLSC increased by 22.62% (34.9%), 10.30% (17.8%), and 9.96% (23.3%) in the three seasons, compared with those under TC. Cultivation method had significant influence on NutE (except 2017–2018 season). The average NutE across three irrigation levels under HLSC was 1.81%, 6.80%, and 11.01% lower than those under TC in the three seasons, respectively.

Table 2
Grain yield and yield components of winter wheat under different cultivation pattern and irrigation level.

Seasons	Cultivation pattern	Irrigation level	Spike number (10^4 ha^{-1})	Kernels per spike	1000-grain weight (g)	Grain yield (kg ha^{-1})
2017–2018	TC	H	557 b	33.30 ab	43.16 a	6686c
	HLSC	H	778 a	32.01 b	43.39 a	8199 a
		M	729 a	32.66 ab	42.34 a	8059 ab
		L	702 a	34.38 a	42.55 a	7909 b
		AVG	**736**	**33.01**	**42.76**	**8056**
2018–2019	TC	H	660 b	40.17 a	47.93 a	8656 bc
		M	630 b	37.92 ab	47.27 b	8332 cd
		L	555c	35.83 b	47.20 b	7815 d
		AVG	**615**	**37.97**	**47.47**	**8268**
	HLSC	H	753 a	36.46 b	48.07 a	9480 a
		M	741 a	35.91 b	48.28 a	9048 ab
		L	674 b	37.26 b	46.67 d	8831 bc
		AVG	**723**	**36.54**	**47.67**	**9120**
2019–2020	TC	H	687 b	25.94 a	49.96c	9283 bc
		M	683 b	24.57 b	50.65 ab	9091 bc
		L	659 b	23.62c	50.91 a	8754c
		AVG	**676**	**24.71**	**50.51**	**9043**
	HLSC	H	852 a	24.88 b	50.28 bc	10147 a
		M	848 a	24.46 b	50.77 ab	9856 ab
		L	825 a	24.74 b	51.08 a	9827 ab
		AVG	**842**	**24.69**	**50.71**	**9944**

Note: AVG means the average of three irrigation levels. The different lowercase letters in the same column indicate significant differences among different treatments at $P < 0.05$ level.

Table 3
Analysis of variance showing the effects of the cultivation pattern, irrigation level and their interaction on the grain yield and yield components of winter wheat in the 2017–2018 – 2019–2020 growing seasons.

ANOVA	2017–2018				2018–2019				2019–2020			
	Spike number (10^4 ha^{-1})	Kernels per spike	1000-grain weight (g)	Grain yield (kg ha^{-1})	Spike number (10^4 ha^{-1})	Kernels per spike	1000-grain weight (g)	Grain yield (kg ha^{-1})	Spike number (10^4 ha^{-1})	Kernels per spike	1000-grain weight (g)	Grain yield (kg ha^{-1})
C	**	NS	NS	**	**	NS	NS	**	**	NS	NS	**
I	NS	*	NS	NS	**	NS	**	**	NS	**	* *	NS
C×I	-	-	-	-	NS	*	**	NS	NS	**	NS	NS

Note: C means cultivation methods, I means irrigation levels, and C×I means the interaction effect of two factors. ** Significant differences at $P < 0.01$; *Significant differences at $P < 0.05$; NS means no significant difference.

Table 4
Analysis of variance showing the effects of the cultivation pattern, irrigation level and their interaction on the evapotranspiration (ET_a, mm), soil water depletion (mm) and water use efficiency (*WUE*, kg m^{-3}) of winter wheat in the 2017–2018 – 2019–2020 growing seasons.

Analysis of variance	2017–2018				2018–2019				2019–2020			
	ET_a	Soil water depletion	WUE_G	WUE_{AB}	ET_a	Soil water depletion	WUE_G	WUE_{AB}	ET_a	Soil water depletion	WUE_G	WUE_{AB}
C	**	**	**	**	**	**	NS	**	**	**	NS	**
I	*	**	*	NS	**	**	NS	**	**	**	NS	NS
C×I	-	-	-	-	**	*	NS	**	NS	NS	NS	NS

Note: C means cultivation methods, I means irrigation levels, and C×I means the interaction effect of two factors. ** Significant differences at $P < 0.01$; *Significant differences at $P < 0.05$; NS means no significant difference.

Table 5
Analysis of variance showing the effects of the cultivation pattern, irrigation level and their interaction on the total nitrogen uptake at maturity (N_t, kg ha^{-1}), nitrogen use efficiency (NUE, kg kg^{-1}), nitrogen uptake efficiency (NupE, kg kg^{-1}) and nitrogen utilization efficiency (NutE, kg kg^{-1}) of winter wheat in the 2017–2018 – 2019–2020 growing seasons.

ANOVA	2017–2018				2018–2019				2019–2020			
	N_t	NUE	NupE	NutE	N_t	NUE	NupE	NutE	N_t	NUE	NupE	NutE
C	**	**	**	NS	**	**	**	**	**	**	**	**
I	NS	NS	NS	NS	**	**	**	NS	NS	NS	NS	NS
C×I	-	-	-	-	NS	NS	NS	NS	NS	NS	NS	NS

Note: C means cultivation methods, I means irrigation levels, and C×I means the interaction effect of two factors. ** Significant differences at $P < 0.01$; *Significant differences at $P < 0.05$; NS means no significant difference.

3.6. Correlation analysis and PCA

As shown in Fig. 6, grain yield was closely related to LAI, shoot biomass, and spike biomass in all three seasons. The correlation between grain yield and LAI, grain yield and shoot biomass was strong, with all R^2 values greater than 0.83. Grain yield increased with the increase of LAI and shoot biomass, which indicated that increasing LAI and biomass was the key to obtaining high yield in winter wheat production.

For yield compositions, the R^2 between grain yield and spike number at harvest was significant (Fig. 6). There was no significant correlation between grain yield and kernels per spike or 1000-grain weight. Therefore, for the three factors of grain composition, more attention should be paid to improving the spike number at harvest for a higher yield. This result also indicated that the higher grain yield under HLSC, compared with those under TC might attribute mainly to the significant improvement in tillering and the remarkable increase of spike number at harvest under HLSC.

Then, PCA was performed on all indexes of winter wheat in the three growing seasons. In this study, three principal components (PC1, PC2 and PC3) were extracted from data in 2017–2018, 2018–2019 and 2019–2020 ($\lambda > 1$) and the eigenvalues (λ) of principal components 1 and 2 (PC1 +PC2) of three seasons were 7.74, 7.28, 7.05, respectively, which explained 85.6%, 80.9% and 78.5%, respectively (Fig. 7). The rankings of comprehensive scores based on the PCA are presented in Table 6. The full irrigation treatment of HLSC ranked first in 2018–2019 and 2019–2020 season, while mild deficit irrigation treatment of HLSC ranked first in 2017–2018 season.

4. Discussion

4.1. Distribution of soil water and NO3-N under different cultivation patterns

Water and nitrogen are two important necessary elements for crop growth. Crops mainly uptake water and nitrogen from the soil, so the spatial distribution of water and nitrogen in the soil profile has a significant impact on crop population development. This study showed that the water content of topsoil in the high bed of HLSC was relatively low even just after irrigation (Fig. 3), compared with that in the low bed of HLSC. Previous studies have shown that soil evaporation is closely related to SWC. The smaller the SWC is, the smaller the soil evaporation (Liao et al., 2021). A previous study indicated that evapotranspiration firstly was supplied by water stored in the top 10 cm of soil, while the process of deep soil moisture passing through the capillary is slower (Berg et al., 2016). Therefore, the lower water content in topsoil in the high bed of HLSC reduced ineffective soil surface evaporation and contributed to the improvement of WUE (Table S5). Except for the topsoil, the SWC in the same depth of soil layer beneath HLSC-H and HLSC-L were nearly the same (Fig. 3). These results indicated that although watering under the HLSC pattern may be considered as local irrigation, the soil water status at same soil layer beneath different seedbeds is not remarkably different by subsequent water infiltration

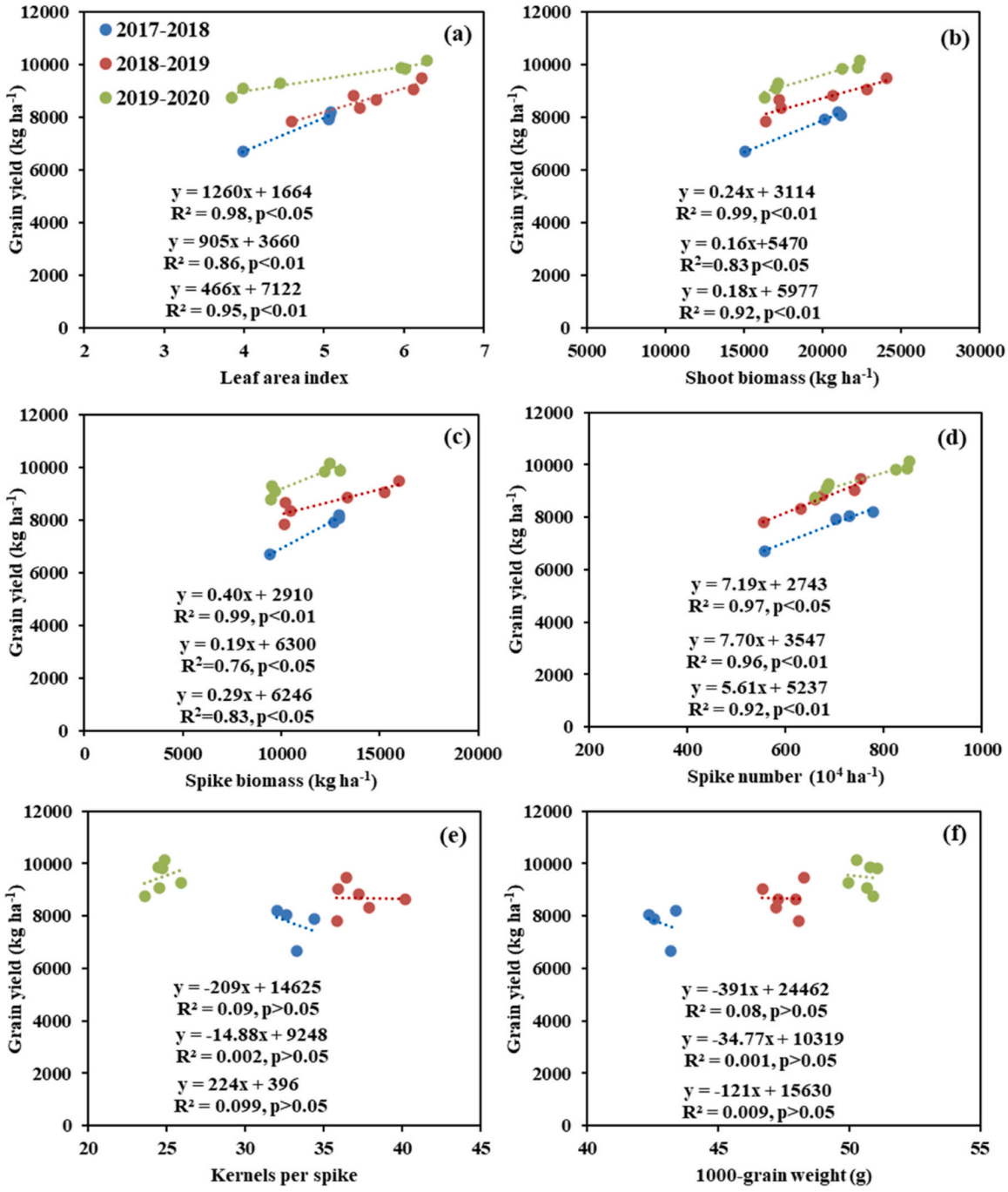

Fig. 6. The correlation between grain yield and growth indices, or yield components of winter wheat in the three wheat seasons.

and redistribution. Therefore, this local irrigation mode has little effect on the water supply for plants requirement on the high bed of the HLSC pattern. However, soil NO_3-N beneath the HLSC-H was significantly lower than those in the same soil layer beneath the HLSC-L (Fig. 4) after topdressing nitrogen fertilizer, and these differences continued until the harvest stage. Several studies have shown that roots have plasticity and obvious growth toward fertility (Grossman and Rice, 2012; Jiang et al., 2017). However, due to the large width of HLSC, wheat roots in raised bed seem to be difficult to extend into the area beneath the low bed and gain enough nitrogen, which may affect the nitrogen uptake and growth of wheat on the raised bed.

4.2. *Winter wheat growth and yield under different cultivation patterns*

Shoot biomass and LAI is two key characteristics of crop growth and development. Studies have shown that wheat grain yield is closely related to LAI and shoot biomass (Shi et al., 2016; Wang et al., 2016). Larger LAI will help produce higher biomass (Man et al., 2017), thus contributing to the increase in winter wheat yield (Xue et al., 2006; Xu et al., 2018). In this study, the LAI and shoot biomass under HLSC were significantly higher than those under TC for different irrigation levels. Due to the higher LAI and aboveground biomass, the grain yield of HLSC was significantly higher than that of TC. HLSC increased the averaged grain yield across irrigation levels by 22.63%, 10.30%, and 9.96%, compared with TC, in the three seasons, respectively. In addition, suitable soil moisture condition is the key to obtaining a high yield of crops.

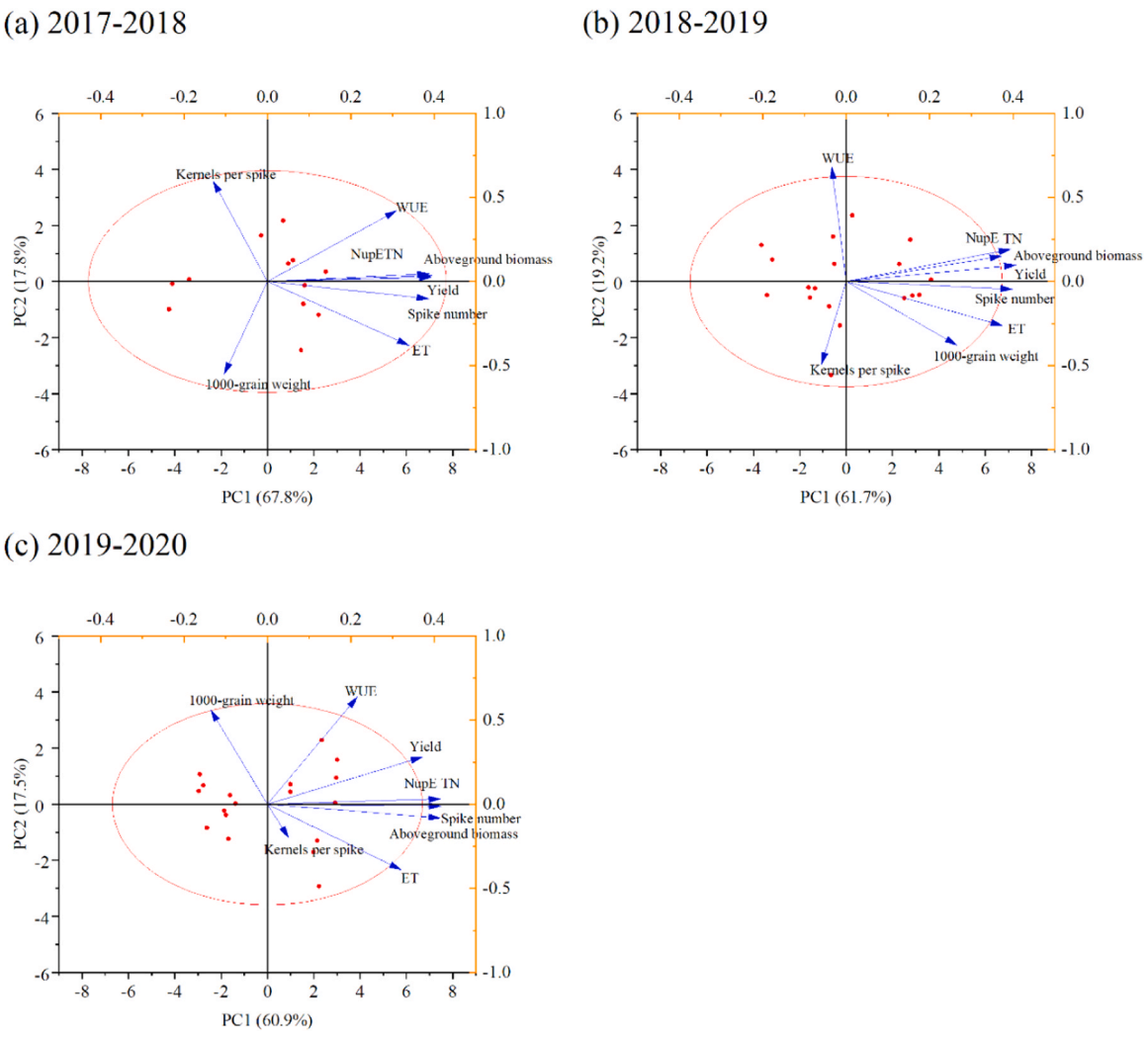

Fig. 7. Principal component analysis of wheat yield, spike number, kernels per spike, 1000-grain weight, aboveground biomass, ET, total nitrogen uptake (TN), water use efficiency (WUE), and nitrogen uptake efficiency (NupE).

Table 6
Comprehensive scores of principal component analysis.

Cultivation pattern	Irrigation level	2017–2018		2018–2019		2019–2020	
		Score	Rank	Score	Rank	Score	Rank
TC	H	-3.17	4	-0.88	4	-1.38	4
	M			-1.23	5	-1.62	5
	L			-2.48	6	-2.07	6
HLSC	H	1.07	2	2.39	1	2.06	1
	M	1.44	1	2.05	2	1.64	2
	L	0.65	3	0.16	3	1.38	3

Note: H, M, and L mean full irrigation, mild deficit irrigation, and deficit irrigation, respectively.

Previous studies showed that the wheat growth and yield components of winter wheat increased with the increase in irrigation amount (Si et al., 2020; You et al., 2022). Consistent results were obtained in this study, showing that LAI, shoot biomass, and grain yield increased with the increase in irrigation amount. Under both cultivation patterns, LAI and aboveground biomass reached their maximum under full irrigation treatment, and finally, the yield reached its maximum under full irrigation treatment.

The analysis results of yield components and correlation analysis indicated that the increase of wheat grain yield under HLSC was mainly the result of an obvious increase in the number of spikes m^{-2} (Table 3; Fig. 6), which was consistent with the results of previous studies (Xu et al., 2018; Si et al., 2020). In this study, because the seeding amount under both cultivation patterns was 120 kg ha^{-1}, there were no significant differences between the basic seedlings under HLSC and TC at the early tillering stage (Fig. 5). After that, the plant population density of HLSC was significantly higher than that of TC under three irrigation levels. By improving the population density of winter wheat, the HLSC pattern showed finally the potential of improving grain yield. However, a new concern may be that increased plant density may lead to more lodging risk in the late season of wheat (Khan et al., 2020; Wang et al., 2015). Fortunately, a previous study experimented with two wheat cultivars, and their results showed that the lodging resistance of wheat plants under HLSC was improved compared with that under TC by reducing the plant height and the center of gravity height (Wu et al., 2021).

Previous studies argued that light is the major resource limiting grain yield, and plant numbers and distribution need to be no more than that necessary to intercept all the radiation, or at least 95% of it, before flag leaf emergence (Fischer et al., 2019; Pelech et al., 2023; Pergner and Lippert, 2023). Experiments conducted in Mexico have shown that the maximum wheat spacing without yield reduction is 44 cm for most dwarf wheat. Based on more than 30 years of research on row spacing, Fischer et al. (2019) concluded that the erect dwarf cultivars lost yield at spacing 30 cm and greater, while some taller vigorous semidwarf cultivars tolerated spacing up to at least 50 cm without yield loss (Fischer

et al., 2019). The TC pattern generally requires wider ridges to restrict irrigation water flowing along the long basin, which will undoubtedly lead to a part of the land that cannot be planted with wheat. In this study, the distance between the two plant rows on both sides of the ridge was 60 cm. The wheat canopy could not fully cover the entire soil surface at late growth stages, which resulted in a loss of light energy at the stage of flag leaf emergence (Fischer et al., 2019). This is considered as a very important reason why the yield of TC is lower than that of HLSC. In addition, the alternative high-beds and low-beds under HLSC formed a "micro-terrace" structure, which is benefitable for improving light interception, ventilation, and photosynthetic rate (Wang et al., 2009; Du et al., 2021b).

4.3. Water and nitrogen use efficiency of wheat under different cultivation patterns

In North China, only about 30% of the annual rainfall occurs during the winter wheat growing season (October–May), which is far less than the water requirements for normal wheat production (Jha et al., 2019; Liu et al., 2023b). However, rainfall is generally abundant in the non-wheat growing period (concentrated from June to September), and a notable part of rainfall is lost as surface runoff or deep leakage, especially after heavy rain. Therefore, it is important to induce wheat roots to uptake more soil water storage, especially more water storage of deep soil layers (Lynch and Wojciechowski, 2015; Fang et al., 2017). In this study, soil water storage in 0–150 cm soil profile under HLSC was significantly lower than that under TC at harvest time, and the difference was mainly manifested in the middle and deep soil layers (Fig. S2). Their results indicated that HLSC induced wheat to uptake more soil water storage, especially in deep soil layers. On the one hand, improving the utilization of soil water storage during the winter wheat season may effectively reduce irrigation demand. On the other hand, the consumption of soil water storage in deep soil layers may empty the water storage space before the summer rainy season and then stores up more rainwater, which benefits able for reducing deep leakage and improving the utilization efficiency of rainfall (Li et al., 2005; Xu et al., 2016).

The total water consumption during the entire wheat growth period under HLSC was significantly higher than that under TC for three irrigation levels (Table S5), which was mainly attributed to greater population density, larger LAI, and significantly higher transpiration of plants under HLSC. Because LAI is an important index to characterize crop canopy and is closely related to crop evapotranspiration (Netzer et al., 2009; Bian et al., 2018). However, the WUE_G and WUE_{AB} of HLSC were significantly higher than those of TC for three irrigation levels (Table S5), indicating that although the HLSC mode consumed more water, it produced higher grain yield and shoot biomass per unit of water consumption. The reasons may be that both raised and low beds under HLSC were planted wheat, and that soil surfaces were fully covered earlier than that under TC. Moreover, the topsoil of the high bed was generally with lower SWC (Fig. 4), which reduced effectively soil surface evaporation and improved the final WUE.

HLSC significantly improved NUE, which inferred that the HLSC pattern result in a higher grain yield per unit input of nitrogen fertilizer (Table 5; Table S6). Previous study revealed that NupE and NutE are two primary components of NUE, respectively representing the efficiency of absorption and the efficiency with which the N absorbed is utilized to produced grain (Moll et al., 1982). In this study, results showed that HLSC pattern was efficient in N uptake in different irrigation level in three seasons, but it was inefficient in utilizing the N taken up in grain production, compared with TC. Therefore, it may be concluded that higher yield and NUE of HLSC derived from higher N uptake efficiency. Increasing irrigation amount had promoted effects on N_t and NUE for both TC and HLSC patterns, indicating the importance of ensuring suitable soil moisture for nitrogen uptake and utilization of winter wheat (Si et al., 2020).

4.4. Evaluate and select the appropriate cultivation pattern

High yield is the ultimate goal for agricultural producers. Meanwhile, high resource use efficiency (i.e., WUE and NUE) are the core components of agricultural sustainable development. In crop production, these indicators are mainly related to crop cultivars (Postma et al., 2021; Liu et al., 2023a), management practices (cultivation, irrigation, fertilization, and plant density) (Jha et al., 2019; Si et al., 2020; Zou et al., 2020; Lai et al., 2022), soil quality (Bünemann et al., 2018; Di Mauro et al., 2018) and climate environment (van Ittersum et al., 2013). Among them, developing the appropriate cultivation pattern is helpful to maximize yield, WUE and NUE (or NupE) at the same time. In the present study, we used the PCA tool to evaluate the yield, WUE and NupE of the six treatments. Previous studies indicated that the PCA tool can provide a comprehensive evaluation of target populations (Li et al., 2021; Abubakar et al., 2022; Huang et al., 2022). PCA revealed the best water and fertilizer schemes in sandy loam soils in Northwest China (Xing et al., 2022).

PCA of this study indicated that full irrigation of HLSC ranked first, and mild irrigation of HLSC ranked second in 2018–2019 and 2019–2020 season (Table 6). In 2017–2018, mild irrigation of HLSC ranked first, full irrigation of HLSC ranked second. HLSC had the highest grain yield, aboveground biomass, NupE and WUE compared to TC. Furthermore, the comprehensive scores of HLSC were higher than those of TC across three irrigation levels. Taken together, HLSC is a promising cultivation pattern for improving grain yield and water-nitrogen use efficiency in winter wheat production in the NCP.

5. Conclusion

The grain yield of winter wheat under HLSC was significantly higher than that under TC for all three irrigation levels. The most important reason was considered that the bare ridge areas under TC were transformed into high beds for wheat planting under HLSC, which improved the land utilization rate and resulted in a significant increase in population density, LAI, and biomass. More soil water storage in subsoil layers could be absorbed and utilized under HLSC, which is helpful to enlarge soil reservoir capacity for storing rainwater in the coming rainy season. The increases of WUE and NUE of wheat under HLSC contributed mainly to the decrease of ineffective soil surface evaporation and the improvement of plants' nitrogen uptake efficiency, respectively. The PCA results revealed that the HLSC are recommended as the best cultivation for improving productivity, and water-nitrogen use efficiency in NCP.

CRediT authorship contribution statement

Zhuanyun Si: Conceptualization, Investigation, Formal analysis, Writing-original draft. Junming Liu: Investigation, Formal analysis, Writing-review & editing. Lifeng Wu: Resources, Writing-review & editing. Sen Li: Writing-review & editing. Guangshuai Wang: Writing-review & editing. Jiachuan Yu: Writing-review & editing. Yang Gao: Conceptualization, Funding acquisition, Writing–review& editing. Aiwang Duan: Conceptualization, Writing-review & editing.

Declaration of Competing Interest

The authors declare that they have no known competing financial interests or personal relationships that could have appeared to influence the work reported in this paper.

Data Availability

Data will be made available on request.

Acknowledgements

We are grateful for the financial support from the Ministry of Finance and Ministry of Agriculture and Rural Affairs of the People's Republic of China (CARS-03–19), the National Natural Science Foundation of China (No. 51879267), the Agricultural Science and Technology Innovation Program (ASTIP), and the Central Public-interest Scientific Institution Basal Research Fund (FIRI2022–16).

Appendix A. Supporting information

Supplementary data associated with this article can be found in the online version at doi:10.1016/j.fcr.2023.109010.

References

Abubakar, S.A., Hamani, A.K.M., Chen, J., Sun, W., Wang, G., Gao, Y., Duan, A., 2022. Optimizing N-fertigation scheduling maintains yield and mitigates global warming potential of winter wheat field in North China Plain. J. Clean. Prod. 357, 131906.
Berg, A., Sheffield, J., Milly, P., 2016. Divergent surface and total soil moisture projections under global warming: future soil moisture changes in CMIP5. Geophys. Res. Lett. 44, 236–244.
Bian, Z., Gu, Y., Zhao, J., Pan, Y., Li, Y., Zeng, C., Wang, L., 2018. Simulation of evapotranspiration based on leaf area index, precipitation and pan evaporation: a case study of Poyang Lake watershed, China. Ecohydrol. Hydrobiol. 19, 83–92.
Bünemann, E.K., Bongiorno, G., Bai, Z., Creamer, R.E., De Deyn, G., de Goede, R., Fleskens, L., Geissen, V., Kuyper, T.W., Mäder, P., Pulleman, M., Sukkel, W., van Groenigen, J.W., Brussaard, L., 2018. Soil quality – a critical review. Soil Biol. Biochem. 120, 105–125.
Cassman, K.G., Grassini, P., 2020. A global perspective on sustainable intensification research. Nat. Sustain. 3, 262–268.
Di Mauro, G., Cipriotti, P.A., Gallo, S., Rotundo, J.L., 2018. Environmental and management variables explain soybean yield gap variability in Central Argentina. Eur. J. Agron. 99, 186–194.
van Dijk, M., Morley, T., Rau, M.-L., Saghai, Y., 2021. A meta-analysis of projected global food demand and population at risk of hunger for the period 2010–2050. Nat. Food 2, 494–501.
Du, T., Kang, S., Zhang, X., Zhang, J., 2014. China's food security is threatened by the unsustainable use of water resources in North and Northwest China. Food Energy Secur. 3, 7–18.
Du, X., He, W., Wang, Z., Xi, M., Xu, Y., Wu, W., Gao, S., Liu, D., Lei, W., Kong, L., 2021a. Raised bed planting educes waterlogging and increases yield in wheat following rice. Field Crops Res. 265, 108119.
Du, X., Wang, Z., Xi, M., Wu, W., Wei, Z., Xu, Y., Yongjin, Z., Lei, W., Kong, L., 2021b. A novel planting pattern increases the grain yield of wheat after rice cultivation by improving radiation resource utilization. Agric. For. Meteorol. 310, 108625.
Fang, Y., Du, Y.-L., Wang, J., Aijiao, W., Qiao, S., Xu, B., Zhang, S., Siddique, K., Chen, Y., 2017. Moderate Drought Stress Affected Root Growth and Grain Yield in Old. Mod. New. Release Cultiv. Winter Wheat. Front. Plant Sci. 8.
Fischer, R.A., Ramos, O.H., Ortiz-Monasterio, I., Sayre, K.D., 2019. Yield response to plant density, row spacing and raised beds in low latitude spring wheat with ample soil resources: An update. Field Crops Res. 232, 95–105.
Grossman, J., Rice, K., 2012. Evolution of root plasticity responses to variation in soil nutrient distribution and concentration. Evolut. Appl. 5, 850–857.
Guarin, J., Martre, P., Ewert, F., Webber, H., Dueri, S., Calderini, D., Reynolds, M., Molero, G., Miralles, D., García, G., Slafer, G., Giunta, F., Pequeno, D., Stella, T., Ahmed, M., Alderman, P., Basso, B., Berger, A., Bindi, M., Asseng, S., 2022. Evidence for increasing global wheat yield potential. Environ. Res. Lett. 17, 124045.
Huang, C., Zhang, W., Wang, H., Gao, Y., Ma, S., Qin, A., Liu, Z., Zhao, B., Ning, D., Zheng, H., Liu, Z., 2022. Effects of waterlogging at different stages on growth and ear quality of waxy maize. Agric. Water Manag. 266, 107603.
van Ittersum, M.K., Cassman, K.G., Grassini, P., Wolf, J., Tittonell, P., Hochman, Z., 2013. Yield gap analysis with local to global relevance—A review. Field Crops Res. 143, 4–17.
Jha, S., Ramatshaba, T.S., Wang, G., Liang, Y., Liu, H., Gao, Y., Duan, A., 2019. Response of growth, yield and water use efficiency of winter wheat to different irrigation methods and scheduling in North China Plain. Agric. Water Manag. 217, 292–302.
Jia, M., Xu, H., Liu, C., Mao, R., Li, H., Liu, J., Du, W., Wang, W., Zhang, X., Han, R., Wang, X., Wu, L., Liang, X., Song, J., He, H., Ma, P., 2020. Characterization of the Powdery Mildew Resistance Gene in the Elite Wheat Cultivar Jimai 23 and Its Application in Marker-Assisted Selection. Front. Genet. 11, 672-672.
Jiang, S., Sun, J., Tian, Z., Hu, H., Michel, E., Gao, J., Jiang, D., Cao, W., Dai, T., 2017. Root extension and nitrate transporter up-regulation induced by nitrogen deficiency improves nitrogen status and plant growth at the seedling stage of winter wheat (Triticum aestivum L.). Environ. Exp. Bot. 141, 28–40.
Khan, A., Ahmad, A., Ali, W., Hussain, S., Ajayo, B., Raza, M., Kamran, M., Te, X., Amin, N., Ali, S., Iqbal, N., Khan, I., Sattar, M., Ali, A., Wu, Y., Yang, W., 2020. Optimization of plant density and nitrogen regimes mitigate lodging risk in wheat (Triticum aestivum L.). Agron. J. 112, 2535–2551.
Lai, Z., Fan, J., Yang, R., Xu, X., Liu, L., Li, S., Zhang, F., Li, Z., 2022. Interactive effects of plant density and nitrogen rate on grain yield, economic benefit, water productivity and nitrogen use efficiency of drip-fertigated maize in northwest China. Agric. Water Manag. 263, 107453.
Li, J., Inanaga, S., Li, Z., Eneji, A., 2005. Optimizing irrigation scheduling for winter wheat in the North China Plain. Agric. Water Manag. 76, 8–23.
Li, S., Abdoul Kader, M., Zhang, Y., Liang, Y., Gao, Y., Duan, A., 2021. Coordination of leaf hydraulic, anatomical, and economical traits in tomato seedlings acclimation to long-term drought. BMC Plant Biol. 21, 536-536.
Liao, Y., Cao, H.-X., Liu, X., Li, H.-T., Hu, Q.-Y., Xue, W.-K., 2021. By increasing infiltration and reducing evaporation, mulching can improve the soil water environment and apple yield of orchards in semiarid areas. Agric. Water Manag. 253, 106936.
Liu, G., Yang, Y., Guo, X., Liu, W., Xie, R., Ming, B., Xue, J., Wang, K., Li, S., Hou, P., 2023a. A global analysis of dry matter accumulation and allocation for maize yield breakthrough from 1.0 to 25.0 Mg ha−1. Resour., Conserv. Recycl. 188, 106656.
Liu, J., Gao, Y., Si, Z., Wi, L., Duan, A., 2020. Effects of cultivation methods on water consumption, yield and water use efficiency of winter wheat. J. Soil Water Conserv. 34, 210–216.
Liu, J., Si, Z., Li, S., Kader Mounkaila Hamani, A., Zhang, Y., Wu, L., Gao, Y., Duan, A., 2023b. Variations in water sources used by winter wheat across distinct rainfall years in the North China Plain. J. Hydrol. 618, 129186.
Lynch, J., Wojciechowski, T., 2015. Opportunities and challenges in the subsoil: Pathways to deeper rooted crops. J. Exp. Bot. 2199–2210.
Man, J., Yu, Z., Shi, Y., 2017. Radiation Interception, Chlorophyll Fluorescence and Senescence of Flag leaves in Winter Wheat under Supplemental Irrigation. Sci. Rep. 7, 7767-7713.
Ministry of Water Conservancy, 2017. China statistical yearbook of water resources. Beijing: China WaterPower Press.
Moll, R.H., Kamprath, E.J., Jackson, W.A., 1982. Analysis and interpretation of factors which contribute to efficiency of nitrogen utilization. Agron. J. 74, 562–564.
Netzer, Y., Yao, C., Shenker, M., Bravdo, B.-A., Schwartz, A., 2009. Water use and the development of seasonal crop coefficients for Superior Seedless grapevines trained to an open-gable trellis system. Irrig. Sci. 27, 109–120.
Pelech, E.A., Evers, J.B., Pederson, T.L., Drag, D.W., Fu, P., Bernacchi, C.J., 2023. Leaf, plant, to canopy: A mechanistic study on aboveground plasticity and plant density within a maize–soybean intercrop system for the Midwest, USA. Plant, Cell Environ. 46, 405–421.
Pergner, I., Lippert, C., 2023. On the effects that motivate pesticide use in perspective of designing a cropping system without pesticides but with mineral fertilizer—a review. Agron. Sustain. Dev. 43, 24.
Postma, J.A., Hecht, V.L., Hikosaka, K., Nord, E.A., Pons, T.L., Poorter, H., 2021. Dividing the pie: A quantitative review on plant density responses. Plant. Cell Environ. 44, 1072–1094.
Qi, X., Wang, R., Li, J., Zhang, T., Liu, L., He, Y., 2018. Ensuring food security with lower environmental costs under intensive agricultural land use patterns: A case study from China. J. Environ. Manag. 213, 329–340.
Shi, Y., Yu, Z., Man, J., ma, S., Gao, Z., Zhang, Y., 2016. Tillage practices affect dry matter accumulation and grain yield in winter wheat in the North China Plain. Soil Tillage Res. 160, 73–81.
Si, Z., Zain, M., Mehmood, F., Wang, G., Gao, Y., Duan, A., 2020. Effects of nitrogen application rate and irrigation regime on growth, yield, and water-nitrogen use efficiency of drip-irrigated winter wheat in the North China Plain. Agric. Water Manag. 231, 106002.
Wang, B., Zhang, Y., Hao, B., Xu, X., Zhao, Z., Wang, Z., Xue, Q., 2016. Grain Yield and Water Use Efficiency in Extremely-Late Sown Winter Wheat Cultivars under Two Irrigation Regimes in the North China Plain. Plos One 11, e0153695.
Wang, C., Ruan, R., Yuan, X., Hu, D., Yang, H., Li, Y., Yi, Z., 2015. Effects of Nitrogen Fertilizer and Planting Density on the Lignin Synthesis in the Culm in Relation to Lodging Resistance of Buckwheat. Plant Prod. Sci. 18, 218–227.
Wang, F., Wang, X., Sayre, K., 2004. Comparison of conventional, flood irrigated, flat planting with furrow irrigated, raised bed planting for winter wheat in China. Field Crops Res. 87, 35–42.
Wang, F., He, Z., Sayre, K., Li, S., Si, J., Feng, B., Kong, L., 2009. Wheat cropping systems and technologies in China. Field Crops Res. 111, 181–188.
Wu, L., Han, X., Islam, S., Zhai, S., Zhao, H., Zhang, G., Cui, G., Zhang, F., Han, W., You, X., Ju, Z., Lv, P., Zhou, J., Gao, Q., Cui, B., Wu, Y., Yang, Z., Liu, Q., Yang, F., Zhang, J., Liu, H., 2021. Effects of Sowing Mode on Lodging Resistance and Grain Yield in Winter Wheat. Agronomy 11, 1378.
Xing, Y., Zhang, T., Jiang, W., Li, P., Shi, P., Xu, G., Cheng, S., Cheng, Y., Fan, Z., Wang, X., 2022. Effects of irrigation and fertilization on different potato varieties growth, yield and resources use efficiency in the Northwest China. Agric. Water Manag. 261, 107351.
Xu, C., Tao, H., Tian, B., Gao, Y., Ren, J., Wang, P., 2016. Limited-irrigation improves water use efficiency and soil reservoir capacity through regulating root and canopy growth of winter wheat. Field Crops Res. 196.
Xu, X., Zhang, M., Li, J., Liu, Z., Zhao, Z., Zhang, Y., Zhou, S., Wang, Z., 2018. Improving water use efficiency and grain yield of winter wheat by optimizing irrigations in the North China Plain. Field Crops Res. 221, 219–227.
Xue, Q., Zhu, Z., Musick, J., Stewart, B., Dusek, D., 2006. Physiological mechanisms contributing to the increased water-use efficiency in winter wheat under deficit irrigation. J. Plant Physiol. 163, 154–164.

You, Y., Song, P., Yang, X., Zheng, Y., Dong, L., Chen, J., 2022. Optimizing irrigation for winter wheat to maximize yield and maintain high-efficient water use in a semi-arid environment. Agric. Water Manag. 273, 107901.
Zhang, C., Dong, Z., Guo, Q., Hu, Z., Li, J., Wei, T., Ding, R., Cai, T., Ren, X., Han, Q., Zhang, P., Jia, Z., 2022. Ridge–furrow rainwater harvesting combined with supplementary irrigation: Water-saving and yield-maintaining mode for winter wheat in a semiarid region based on 8-year in-situ experiment. Agric. Water Manag. 259, 107239.
Zou, H., Fan, J., Zhang, F., Xiang, Y., Wu, L., Yan, S., 2020. Optimization of drip irrigation and fertilization regimes for high grain yield, crop water productivity and economic benefits of spring maize in Northwest China. Agric. Water Manag. 230, 105986.